# Multiconfiguration Pair-Density Functional Theory for Iron Porphyrin with CAS, RAS, and DMRG Active Spaces

Chen Zhou, Laura Gagliardi,* and Donald G. Truhlar*

Department of Chemistry, Chemical Theory Center, and Supercomputing Institute, University of Minnesota, Minneapolis, Minnesota 55455-0431, United States

**S** *Supporting Information*

**ABSTRACT:** Porphyrins are present in many metalloproteins, and they are also important components of a variety of nonbiological functional materials. Furthermore, they are representative of the kind of large, strongly correlated system that is especially difficult for accurate calculations. For example, predicting the order of their spin states has been challenging. Here we study the energetic order of four states (one singlet, two triplets, and one quintet) of iron porphyrin, FeP, by the multiconfiguration pair-density functional theory (MC-PDFT). Five active space prescriptions, namely, CAS(8, 6), CAS(8, 11), CAS(16, 15), RAS(34,2,2;13,6,16), and DMRG(34, 35), are used to obtain the kinetic energy, density, and on-top density. Although the prediction of which spin state of FeP is the ground state depends on the selection of the active space when one uses multireference second-order perturbation theory and such calculations lead incorrectly to a quintet ground state with the largest studied active space, all five active spaces correctly lead to a triplet ground state when one uses MC-PDFT. We conclude that the (34,35) active space is large enough to give a qualitatively correct description of the orbital space and configuration space such that one obtains the correct spin state prediction when the external correlation energy is added accurately in a post-SCF step. We also conclude that MC-PDFT can provide an efficient and accurate approach to treat the electron correlation in large, strongly correlated systems with the complexity of iron porphyrin.

**MC-PDFT**

$^1A_{1g}$

$^5A_{1g}$

$^3A_{2g}$     $^3E_g$
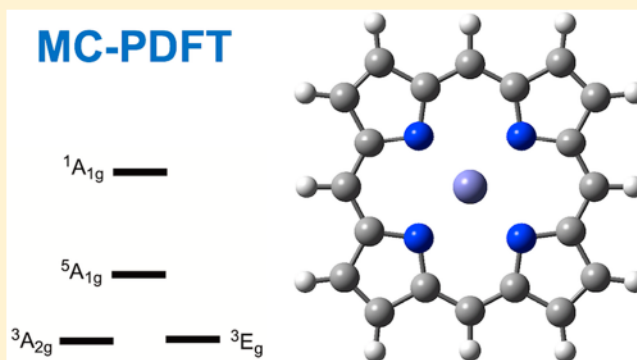
## INTRODUCTION

Iron porphyrin is a prosthetic group in many metalloporphyrins, and it plays an important role in a large number of biological reactions.[1,2] Fe(II) porphyrin complexes have been widely studied by both experiment[3–10] and theory.[11–26] The incomplete d subshell of transition metal atoms and ions such as Fe(II) often leads to low-lying excited spin states, and it is necessary to sort these out to understand the reactivity and chemical properties of transition metal complexes.[27–34] Experiments, including magnetic,[8] Mössbauer,[3,7] proton NMR measurements,[4,9] and Raman spectra,[5] reveal that both tetraphenylporphinatoiron (FeTPP) and octaethylporphinatoiron (FeOEP) molecules possess a triplet ground state. However, determining the correct ground state of even the smaller unsubstituted iron porphyrin (FeP) continues to be challenging.[11]

The FeP molecule has three low-lying spin states, singlet, triplet, and quintet. It has been reported that the ground state is triplet and that correct energetic ordering of the spin states can be obtained with single-reference CCSD(T)[12] and Kohn–Sham density functional theory,[24] although in general one prefers multireference methods for reliable calculations of transition metal spin splittings.[11] The reference wave function for many multireference calculations is complete-active-space

self-consistent field theory (CASSCF),[35] in which the orbitals are optimized for a configuration interaction wave function containing all possible configuration state functions (CSFs) in a chosen active space. For accurate work, external correlation energy, i.e., correlation energy represented by excitations out of the active space, must also be included. However, it has been found when adding external correlation energy by second-order perturbation theory that the energetic order of the low-lying spin states of FeP depends on the choice of active space with the CASPT2[36] method. One possible conventional active space would be 8 active electrons in 11 active orbitals, including five valence d orbitals ("3d orbitals") and five correlating d orbitals ("3d′ orbitals to describe the double shell[37] effect") on the iron atom and one Fe–N σ bonding orbital. Unfortunately, CASPT2 calculations with this choice of active space predict the quintet state to be the ground state by a large margin (0.71 eV).[11]

Such an active space could be enlarged by adding π orbitals of the porphyrin ring, but this leads to 34 active electrons on 35 active orbitals, which puts it beyond the feasibility limit of

conventional CASSCF and CASPT2 calculations. Restricted active-space self-consistent field theory (RASSCF)[38] is an alternative way to treat larger active spaces than are practical with CASSCF calculations. By dividing the active space into RAS1, RAS2, and RAS3 subspaces and restricting the occupation patterns in each subspace, the computational costs can be greatly reduced and larger active spaces become affordable.

Multiconfiguration pair-density functional theory (MC-PDFT)[39,40] is an efficient multiconfiguration method that includes both internal and external correlation energy without calculating them separately. In MC-PDFT, the energy is evaluated using the kinetic energy, the density, and the on-top density of a multiconfiguration wave function. MC-PDFT has been applied to varieties of molecular systems and usually shows high accuracy.[41−44] Recently, we have shown[45] that MC-PDFT may be combined with very large MCSCF wave functions obtained by the density matrix renormalization group[46−51] (DMRG), which allows for much larger active spaces than conventional CASSCF and RASSCF algorithms. The combinations of CASSCF, RASSCF, and DMRG with PDFT will be, respectively, called CAS-PDFT, RAS-PDFT, and DMRG-PDFT. We note that another approach to combining the advantages of DMRG and DFT is the work of Hedegård et al.,[52] who combined single-configuration DFT for short interelectronic separations with complete-active-space DMRG for long interelectronic separations.

Here we present a study of FeP with CAS-PDFT, RAS-PDFT, and DMRG-PDFT to show that DMRG-PDFT calculations allow the use of large active spaces and to see the computational performance of MC-PDFT with different sizes of active spaces. In particular, we study the performance of various methods with respect to whether they get the state ordering correct.

## ■ COMPUTATIONAL DETAILS

The FeP molecule has $D_{4h}$ symmetry, and we study the $^1A_{1g}$, $^3A_{2g}$, $^3E_g$, and $^5A_{1g}$ states with $D_{2h}$ symmetry enforced. The states are identified in Table 1 by the occupancies of the iron 3d orbitals. The available experiments show that the ground state is a triplet,[3−5] but they are not definitive as to whether it is $^3A_{2g}$ or $^3E_g$.

**Table 1. Electron Configurations of the Spin States of FeP**

| state | configuration |
|---|---|
| $^1A_{1g}$ | $(d_{x^2-y^2})^2(d_{z^2})^0(d_{xz},d_{yz})^4$ |
| $^3A_{2g}$ | $(d_{x^2-y^2})^2(d_{z^2})^2(d_{xz},d_{yz})^2$ |
| $^3E_g$ | $(d_{x^2-y^2})^2(d_{z^2})^1(d_{xz},d_{yz})^3$ |
| $^5A_{1g}$ | $(d_{x^2-y^2})^1(d_{z^2})^2(d_{xz},d_{yz})^2(d_{xy})^1$ |

We use the ANO-RCC basis[53,54] contracted to [7s6p5d3f2g1h] for Fe, to [4s3p2d1f] for C and N, and to [3s1p] for H. (This is the same basis set as used in refs 11 and 21.) We use the second-order Douglas−Kroll−Hess (DKH)[55] approximation to include scalar relativistic effects. Geometries for each of the states are taken from ref 21. Cholesky decomposition is used to decompose two-electron integrals with a threshold of $10^{-6}$.

All of the calculations are performed with the *OpenMolcas* 8.3 software package[56,57] with our previously reported implementation[45] of DMRG-PDFT. The DMRG calculations

are performed with the *QCMaquis* software suite[58−61] in *OpenMolcas* 8.3. The calculations are steered by the settings and warm-up procedures of the *QCMaquis* program.[62]

## ■ RESULTS AND DISCUSSION

The active spaces considered, namely, CAS(8, 6), CAS(8, 11), CAS(16, 15), RAS(34,2,2;13,6,16), and DMRG(34, 35), are listed in the first column of Table 2. The smallest active space (8, 6) is obtained by removing the five 3d′ orbitals of the (8, 11) active space (which is explained above). The active space with 16 elections on 15 orbitals is an extension of the (8, 11) space by adding all subvalence 3s and 3p orbitals of the iron atom. The (34,35) active orbital space used in the RAS-(34,2,2;13,6,16) and DMRG(34, 35) calculations is explained above.

The RAS(34,2,2;13,6,16) active space has the same active orbital space as a CAS(34, 35) active space, but it differs in which configuration state functions are included. The configurations included are determined by the partition into RAS1, RAS2, and RAS3 subspaces. The selection of RAS1, RAS2, and RAS3 subspaces made here is the same as in ref 11. Following the notation in ref 11, RAS($n,l,m;i,j,k$) active space contains $n$ active electrons and allows a maximum number of $l$ holes in RAS1 and a maximum of $m$ particles in RAS3. The numbers of orbitals in RAS1, RAS2, and RAS3 are $i$, $j$, and $k$, respectively. Note that the 3s and 3p orbitals of the iron atom are not included in the RAS(34,2,2;13,6,16) or DMRG(34, 35) calculations. The RASSCF calculations involved 849 651, 1 525 365, 1 543 829, and 876 568 CSFs for the $^1A_{1g}$, $^3A_{2g}$, $^3E_g$, and $^5A_{1g}$ states in $D_{2h}$ symmetry.

The (34, 35) active orbital space is also studied with the DMRG method. The DMRG wave function is expanded in matrix product states (MPS),[63] and the expansion is limited by the bond dimension $M$. The exact CASSCF energy for a given active space would be reached if DMRG were applied with a large enough (i.e., converged) bond dimension, and we therefore tested three values of $M$ to show convergence. The configuration interaction dynamically extended active space (CI-DEAS) protocol[64,65] is used to produce the initial MPS for the DMRG calculation.

The active orbitals of the four states are similar for each active space, and they are illustrated in the Supporting Information by giving the active orbitals of the $^3A_{2g}$ state from the RAS(34, 35) calculation and those of $^5A_{1g}$ state from CAS(8, 11) calculation. The Supporting Information also gives two sample input files, including geometries and guess orbitals.

MC-PDFT calculations require the choice of an on-top density functional, and we present results for two choices: tPBE[39] and ftPBE.[42]

Table 2 gives the calculated energies for the four considered states with various methods that we have explained, with both on-top density functionals and with three values of bond dimension in the case of the DMRG calculations. Table 2 also compares the MC-PDFT results to calculations with multi-reference perturbation theory.

RASPT2 calculations with the (34,35) active space, like the CASPT2 calculations with an (8,11) active space, incorrectly predict a quintet ground state.[11] The only CASPT2 or RASPT2 calculations that predict a triplet ground state are those performed with an active space of 16 electrons on 15 orbitals.[11]

Although the small (8,6) active space contains no double-shell effect, CAS-PDFT calculations with the (8,6) active space

**Table 2. Relative Energies (in eV) of the Four States of FeP[a,b]**

| active space | method | $^1A_{1g}$ | $^3A_{2g}$ | $^3E_g$ | $^5A_{1g}$ |
|---|---|---|---|---|---|
| (8, 6) | CASSCF | 2.41 | 1.18 | 1.21 | **0.00** |
| | CAS-PDFT:tPBE | 1.25 | **0.00** | 0.04 | 0.05 |
| | CAS-PDFT:ftPBE | 0.99 | 0.03 | **0.00** | 0.36 |
| (8, 11) | CASSCF | 2.05 | 0.71 | 0.80 | **0.00** |
| | CASPT2[a] | 1.73 | 0.21 | 0.30 | **0.00** |
| | CAS-PDFT:tPBE | 1.03 | **0.00** | 0.05 | 0.36 |
| | CAS-PDFT:ftPBE | 0.82 | **0.00** | 0.01 | 0.62 |
| (16, 15) | CASSCF | 1.56 | 0.54 | 0.64 | **0.00** |
| | CASPT2[a] | 1.30 | **0.00** | 0.10 | 0.04 |
| | CAS-PDFT:tPBE | 1.26 | **0.00** | 0.03 | 0.39 |
| | CAS-PDFT:ftPBE | 1.17 | **0.00** | 0.00 | 0.56 |
| (34,2,2; 13,6,16)[c] | RASSCF | 2.18 | 0.87 | 0.93 | **0.00** |
| | RASPT2[a] | 1.50 | 0.20 | 0.29 | **0.00** |
| | RAS-PDFT:tPBE | 1.31 | **0.00** | 0.08 | 0.37 |
| | RAS-PDFT:ftPBE | 1.12 | **0.00** | 0.04 | 0.63 |
| (34,35) | DMRG($M$ = 100) | 1.99 | 0.83 | 0.95 | **0.00** |
| | DMRG($M$ = 200) | 1.91 | 0.80 | 0.90 | **0.00** |
| | DMRG($M$ = 300) | 1.92 | 0.78 | 0.87 | **0.00** |
| | DMRG-PDFT:tPBE ($M$ = 100) | 1.22 | **0.00** | 0.01 | 0.38 |
| | DMRG-PDFT:tPBE ($M$ = 200) | 1.26 | **0.00** | 0.02 | 0.42 |
| | DMRG-PDFT:tPBE ($M$ = 300) | 1.22 | **0.00** | 0.02 | 0.42 |
| | DMRG-PDFT:ftPBE ($M$ = 100) | 1.04 | 0.03 | **0.00** | 0.68 |
| | DMRG-PDFT:ftPBE ($M$ = 200) | 1.07 | 0.02 | **0.00** | 0.70 |
| | DMRG-PDFT:ftPBE ($M$ = 300) | 1.04 | 0.02 | **0.00** | 0.70 |

[a]All energies are relative to energy of the lowest energy state (which is in bold font) for that line of the table. [b]The CASPT2 and RASPT2 results are taken from ref 11. [c]The (34,2,2;13,6,16) notation is explained in the text; note that this is a restricted active space with the same number of electrons (34) and orbitals (35) as the CAS (34,35) case, but the intersubspace excitations are restricted to a maximum of two holes in RAS1 and a maximum of two particles in RAS3.

**Table 3. DMRG-SCF, DMRG-cu(4)-CASPT2, and DMRG-PDFT Energy (in kcal/mol) for the Four States of FeP with Various Values of $M$ When Using the (8,11) Active Space[a]**

| | $^1A_{1g}$ | | | $^3A_{2g}$ | | | $^3E_g$ | | |
|---|---|---|---|---|---|---|---|---|---|
| $M$ | SCF | PDFT | PT2[b] | SCF | PDFT | PT2[b] | SCF | PDFT | PT2[b] |
| 10 | 48.9 | 14.8 | 42.1 | 17.3 | −9.0 | 6.3 | 20.1 | −6.7 | 8.7 |
| 20 | 47.5 | 15.3 | 41.2 | 16.8 | −8.6 | 5.2 | 19.0 | −7.2 | 7.4 |
| 30 | 47.3 | 15.4 | 40.0 | 16.5 | −8.4 | 5.1 | 18.7 | −7.2 | 7.1 |
| 40 | 47.3 | 15.4 | 39.8 | 16.5 | −8.3 | 5.1 | 18.6 | −7.1 | 6.9 |
| 50 | 47.3 | 15.4 | 39.8 | 16.5 | −8.4 | 5.0 | 18.6 | −7.2 | 6.9 |
| 100 | 47.2 | 15.4 | 39.8 | 16.4 | −8.3 | 5.0 | 18.5 | −7.1 | 6.9 |
| 400 | 47.2 | 15.4 | 39.8 | 16.4 | −8.3 | 4.9 | 18.5 | −7.1 | 7.0 |
| 800 | 47.2 | 15.4 | 39.8 | 16.4 | −8.3 | 5.0 | 18.5 | −7.1 | 6.9 |
| 1000 | 47.2 | 15.4 | 39.8 | 16.4 | −8.3 | 4.9 | 18.5 | −7.1 | 6.9 |

[a]The energy for each state is compared with that of the $^5A_{1g}$ state calculated with the same method and $M$. The tPBE functional is used for DMRG-PDFT. [b]The DMRG-CASPT2 results are taken from ref 21.

correctly predict that the ground state is a triplet. With the tPBE functional, the $^3A_{2g}$ ground state has a slightly lower energy (0.05 eV) than the $^5A_{1g}$ state. The $^3E_g$ is predicted to be the ground state for ftPBE, with an energy 0.36 eV lower than the $^5A_{1g}$ state. Note that the energies of the $^3A_{2g}$ and $^3E_g$ states are quite close in CAS-PDFT calculations, and both triplet states are more stable than the quintet state.

For the more commonly used (8,11) active space, the $^5A_{1g}$ state is predicted to be the ground state by both CASSCF and CASPT2. However, in CAS-PDFT, both the tPBE functional and the ftPBE functional correctly give the triplet as the ground state.

When the 3s and 3p orbitals are added to form a (16, 15) active space, the energy of the $^3A_{2g}$ state is slightly lower than

the quintet by CASPT2 calculations,[11] confirming the importance of intershell correlation effects[66] in CASPT2 calculations. This is the only active space for which CASPT2 correctly predicts a triplet ground state. CAS-PDFT also predicts the triplet ground state to be state $^3A_{2g}$ with this active space. Table 2 shows that the energy gaps between the quintet and the triplet states are quite close for the (16, 15) and (8, 11) active spaces.

If all of the $\pi$ electrons are considered, the active orbital space becomes (34, 35), which is not affordable for conventional CASSCF and a following CASPT2 calculation. A RASPT2 calculation in (34, 35) active orbital space was performed by Pierloot et al., but even with such a large active space, RASPT2 predicts the $^5A_{1g}$ state to be the ground state,[11]

as shown in Table 2. However, by using the same RAS space in MC-PDFT, the triplet is correctly predicted to be the ground state. The energy of the $^3A_{2g}$ state is 0.37 and 0.63 eV lower than the $^5A_{1g}$ one for the tPBE and ftPBE functionals, respectively; these values are quite close to the gaps in (8, 11) and (16, 15) active space.

To further test the performance of MC-PDFT with the (34, 35) active orbital space, a DMRG-CASSCF wave function was calculated. This is the same active orbital space as used in the RASSCF calculations. Because the DMRG calculation is done in the CASSCF formalism, it removes the interspace restrictions of the RAS calculations. We used values of 100, 200, and 300 for bond dimension $M$ in this study, and we found that the results for $M = 100$ agree with those for $M = 200$ and 300 to within 0.01–0.04 eV, depending on the case considered.

In many cases, DMRG-CASPT2 are carried out with a large value for $M$ to ensure accuracy; for example, ref 21 used values up to $M = 1000$. Reference 21 also tested an approximation to DMRG-CASPT2 called DMRG-cu(4)-CASPT2. In this method, the 4-particle reduced density matrix is not computed directly but rather is estimated from the 3-particle reduced density matrix to reduce the cost scaling from $a^8$ to $a^6$, where $a$ is the number of active orbitals. In order to provide an indication of the relative convergence rates of PDFT and PT2 with respect to $M$, Table 3 compares our DMRG-PDFT energy for the studied four states of FeP with various values of $M$ in (8,11) active space to the DMRG-cu(4)-CASPT2[21] calculations of ref 21; the table also shows the DMRG-SCF results without external correlation. The table shows that the energy gaps between different spin states converge more rapidly for DMRG-PDFT than for DMRG-cu(4)-CASPT2; in particular, the DMRG-PDFT gaps are within 0.4–0.7 kcal/mol of the converged ones for $M = 10$, where the gaps for DMRG-SCF are unconverged by 0.9–1.7 kcal/mol and those for DMRG-cu(4)-CASPT2 are unconverged by 1.4–2.3 kcal/mol. The stability of the PDFT results in the 100–1000 range of $M$ is a further indication that the bond dimension used in this study is sufficiently large for FeP.

The DMRG-PDFT calculations show that all values used for $M$ in this study yield the triplet as the ground state. When tPBE is used, the $^3A_{2g}$ state is the ground state, while the $^3E_g$ state is predicted as the ground state with the ftPBE functional. Although different triplet states are obtained for the two types of functionals, the energies of $^3A_{2g}$ and $^3E_g$ states are quite close (within 0.01–0.03 eV, depending on the case considered).

## CONCLUSIONS

There are three main conclusions.

(1) The use of DMRG-CASSCF allows a large complete active space employed for FeP. To perform a conventional CASSCF calculation with this active space, the number of CSFs would be $2.2 \times 10^{18}$, $5.2 \times 10^{18}$, and $5.7 \times 10^{18}$ for the singlet, triplet, and quintet, respectively (without using spatial symmetry).

(2) Even with this large complete active space, external correlation energy is needed to get quantitative results. DMRG is a powerful method, but for large molecules it is not sufficient on its own. When DMRG is used to approximate CASSCF wave functions with larger active spaces than can be handled by conventional methods,

the active space might be too large to perform DMRG-CASPT2[21,49] or DMRG-NEVPT2.[59,67,68] Using DMRG in conjunction with PDFT is, however, a powerful way to compute energies that approximate the full correlation energy, not just the internal correlation contained in the active space.

(3) MC-PDFT yields a triplet ground state for all five choices of active space: CAS(8,6), CAS(8, 11), CAS-(16,15), and RAS (34,2,2;13,6,16) and the CAS(34,35) active space used for DMRG. The quintet–triplet energy gap has only a small variation between the four largest active spaces, which demonstrates the stability of MC-PDFT. The CASPT2 and RASPT2 calculations for FeP depend on the active space, and they correctly predict a ground state of triplet for only one of the active spaces employed (16 active electrons on 15 active orbitals). Thus, we see that the DMRG-PDFT calculations are more accurate than CASPT2, which furthermore is not affordable for the largest active space.

The finding that MC-PDFT provides an efficient and accurate approach to treat electron correlation in the iron porphyrin systems is very encouraging for large transition metal complexes in general.

## ASSOCIATED CONTENT

**Ⓢ Supporting Information**

The Supporting Information is available free of charge on the ACS Publications website at DOI: 10.1021/acs.jpca.8b12479.

Absolute energy in hartrees of MSCSF and MC-PDFT calculations; sample input files and active orbitals (including geometry and guess orbitals) (PDF)

## AUTHOR INFORMATION

**Corresponding Authors**
*E-mail: gagliard@umn.edu.
*E-mail: truhlar@umn.edu.

**ORCID** Ⓞ
Chen Zhou: 0000-0002-6332-4198
Laura Gagliardi: 0000-0001-5227-1396
Donald G. Truhlar: 0000-0002-7742-7294

**Notes**
The authors declare no competing financial interest.

## REFERENCES

(1) Meunier, B.; de Visser, S. P.; Shaik, S. Mechanism of oxidation reactions catalyzed by cytochrome P450 enzymes. *Chem. Rev.* 2004, 104, 3947–3980.

(2) Walker, F. A.; Simonis, U. Iron porphyrin chemistry. In *Encyclopedia of Inorganic Chemisry*; Scott, R. A., Ed.; Wiley: New York, 2006.

(3) Collman, J. P.; Hoard, J.; Kim, N.; Lang, G.; Reed, C. A. Synthesis, stereochemistry, and structure-related properties of α, β, γ, δ-tetraphenylporphinatoiron (II). *J. Am. Chem. Soc.* 1975, 97, 2676–2681.

(4) Goff, H.; La Mar, G. N.; Reed, C. A. Nuclear magnetic resonance investigation of magnetic and electronic properties of″ intermediate spin″ ferrous porphyrin complexes. *J. Am. Chem. Soc.* 1977, 99, 3641–3646.

(5) Kitagawa, T.; Teraoka, J. The resonance Raman spectra of intermediate-spin ferrous porphyrin. *Chem. Phys. Lett.* 1979, 63, 443–446.

(6) Dolphin, D.; Sams, J. R.; Tsin, T. B.; Wong, K. L. Synthesis and Mössbauer spectra of octaethylporphyrin ferrous complexes. *J. Am. Chem. Soc.* 1976, 98, 6970–6975.

(7) Lang, G.; Spartalian, K.; Reed, C. A.; Collman, J. P. Mössbauer effect study of the magnetic properties of S = 1 ferrous tetraphenylporphyrin. *J. Chem. Phys.* 1978, 69, 5424–5427.

(8) Boyd, P. D.; Buckingham, D. A.; McMeeking, R. F.; Mitra, S. Paramagnetic anisotropy, average magnetic susceptibility, and electronic structure of intermediate-spin S = 1 (5, 10, 15, 20-tetraphenylporphyrin) iron (II). *Inorg. Chem.* 1979, 18, 3585–3591.

(9) Mispelter, J.; Momenteau, M.; Lhoste, J. M. Proton magnetic resonance characterization of the intermediate (S = 1) spin state of ferrous porphyrins. *J. Chem. Phys.* 1980, 72, 1003–1012.

(10) Strauss, S. H.; Silver, M. E.; Long, K. M.; Thompson, R. G.; Hudgens, R. A.; Spartalian, K.; Ibers, J. A. Comparison of the molecular and electronic structures of (2, 3, 7, 8, 12, 13, 17, 18-octaethylporphyrinato) iron (II) and (trans-7, 8-dihydro-2, 3, 7, 8, 12, 13, 17, 18-octaethylporphyrinato) iron (II). *J. Am. Chem. Soc.* 1985, 107, 4207–4215.

(11) Vancoillie, S.; Zhao, H.; Tran, V. T.; Hendrickx, M. F. A.; Pierloot, K. Multiconfigurational Second-Order Perturbation Theory Restricted Active Space (RASPT2) Studies on Mononuclear First-Row Transition-Metal Systems. *J. Chem. Theory Comput.* 2011, 7, 3961–3977.

(12) Radoń, M. Spin-State Energetics of Heme-Related Models from DFT and Coupled Cluster Calculations. *J. Chem. Theory Comput.* 2014, 10, 2306–2321.

(13) Li Manni, G.; Smart, S. D.; Alavi, A. Combining the complete active space self-consistent field method and the Full Configuration Interaction Quantum Monte Carlo within a super-CI framework, with application to challenging metal-porphyrins. *J. Chem. Theory Comput.* 2016, 12 (3), 1245–1258.

(14) Liao, M.-S.; Scheiner, S. Electronic structure and bonding in metal porphyrins, metal = Fe, Co, Ni, Cu, Zn. *J. Chem. Phys.* 2002, 117, 205–219.

(15) Pierloot, K. The CASPT2 method in inorganic electronic spectroscopy: from ionic transition metal to covalent actinide complexes*. *Mol. Phys.* 2003, 101, 2083–2094.

(16) Li Manni, G.; Alavi, A. Understanding the mechanism stabilizing intermediate spin states in Fe(II)-Porphyrin. *J. Phys. Chem. A* 2018, 122 (22), 4935–4947.

(17) Groenhof, A. R.; Swart, M.; Ehlers, A. W.; Lammertsma, K. Electronic ground states of iron porphyrin and of the first species in the catalytic reaction cycle of cytochrome P450s. *J. Phys. Chem. A* 2005, 109, 3411–3417.

(18) Liao, M.-S.; Watts, J. D.; Huang, M.-J. Electronic Structure of some substituted iron(II) porphyrins. Are they intermediate or high spin? *J. Phys. Chem. A* 2007, 111, 5927–5935.

(19) Radoń, M.; Pierloot, K. Binding of CO, NO, and $O_2$ to Heme by Density Functional and Multireference ab Initio Calculations. *J. Phys. Chem. A* 2008, 112, 11824–11832.

(20) Khvostichenko, D.; Choi, A.; Boulatov, R. Density functional theory calculations of the lowest energy quintet and triplet states of model hemes: Role of functional, basis set, and zero-point energy corrections. *J. Phys. Chem. A* 2008, 112, 3700–3711.

(21) Phung, Q. M.; Wouters, S.; Pierloot, K. Cumulant approximated second-order perturbation theory based on the density matrix renormalization group for transition metal complexes: A benchmark study. *J. Chem. Theory Comput.* 2016, 12, 4352–4361.

(22) Radoń, M.; Broclawik, E.; Pierloot, K. DFT and ab initio study of iron-oxo porphyrins: May they have a low-lying iron(V)-oxo electromer? *J. Chem. Theory Comput.* 2011, 7, 898–908.

(23) Saitow, M.; Kurashige, Y.; Yanai, T. Fully internally contracted multireference configuration interaction theory using density matrix renormalization group: A reduced-scaling implementation derived by computer-aided tensor factorization. *J. Chem. Theory Comput.* 2015, 11, 5120–5131.

(24) Ali, M. E.; Sanyal, B.; Oppeneer, P. M. Electronic structure, spin-states, and spin-crossover reaction of heme-related Fe-porphyrins: A theoretical perspective. *J. Phys. Chem. B* 2012, 116, 5849–5859.

(25) Smith, J. E. T.; Mussard, B.; Holmes, A. A.; Sharma, S. Cheap and Near Exact CASSCF with Large Active Spaces. *J. Chem. Theory Comput.* 2017, 13, 5468–5478.

(26) Phung, Q. M.; Feldt, M.; Harvey, J. N.; Pierloot, K. Toward highly accurate spin state energetics in first-row transition metal complexes: A combined CASPT2/CC approach. *J. Chem. Theory Comput.* 2018, 14, 2446–2455.

(27) In *Spin States in Biochemistry and Inorganic Chemistry: Influence on Structure and Reactivity*; Swart, M., Costas, M., Eds.; Wiley: Oxford, 2015.

(28) Mandal, D.; Shaik, S. Interplay of tunneling, two-state reactivity, and Bell-Evans-Polanyi effects in C-H activation by nonheme Fe(IV)O oxidants. *J. Am. Chem. Soc.* 2016, 138, 2094–2097.

(29) Swart, M.; Gruden, M. Spinning around in transition-metal chemistry. *Acc. Chem. Res.* 2016, 49, 2690–2697.

(30) Ashley, D. C.; Jakubikova, E. Ironing out the photochemical and spin-crossover behavior of Fe(II) coordination compounds with computational chemistry. *Coord. Chem. Rev.* 2017, 337, 97–111.

(31) Verma, P.; Varga, Z.; Klein, J. E. M. N.; Cramer, C. J.; Que, L.; Truhlar, D. G. Assessment of electronic structure methods for the determination of the ground spin states of Fe(II), Fe(III) and Fe(IV) complexes. *Phys. Chem. Chem. Phys.* 2017, 19, 13049–13069.

(32) Gani, T. Z. H.; Kulik, H. J. Unifying exchange sensitivity in transition-metal spin-state ordering and catalysis through bond valence metrics. *J. Chem. Theory Comput.* 2017, 13, 5443–5457.

(33) Wilbraham, L.; Verma, P.; Truhlar, D. G.; Gagliardi, L.; Ciofini, I. (2017). Multiconfiguration pair-density functional theory predicts spin-state ordering in iron complexes with the same accuracy as complete active space second-order perturbation theory at a significantly reduced computational cost. *J. Phys. Chem. Lett.* 2017, 8, 2026–2030.

(34) Grofe, A.; Chen, X.; Liu, W.; Gao, J. Spin-multiplet components and energy splittings by multistate density functional theory. *J. Phys. Chem. Lett.* 2017, 8, 4838–4845.

(35) Roos, B. O.; Taylor, P. R.; Siegbahn, P. E. M. A complete active space SCF method (CASSCF) using a density matrix formulated super-CI approach. *Chem. Phys.* 1980, 48, 157–173.

(36) Andersson, K.; Malmqvist, P. Å.; Roos, B. O. Second-order perturbation theory with a complete active space self-consistent field reference function. *J. Chem. Phys.* 1992, 96, 1218–1226.

(37) Andersson, K.; Roos, B. O. Excitation energies in the nickel atom studied with the complete active space SCF method and second-order perturbation theory. *Chem. Phys. Lett.* 1992, 191, 507–514.

(38) Malmqvist, P. Å.; Pierloot, K.; Shahi, A. R. M.; Cramer, C. J.; Gagliardi, L. The restricted active space followed by second-order perturbation theory method: Theory and application to the study of $CuO_2$ and $Cu_2O_2$ systems. *J. Chem. Phys.* 2008, 128, 204109.

(39) Li Manni, G.; Carlson, R. K.; Luo, S.; Ma, D.; Olsen, J.; Truhlar, D. G.; Gagliardi, L. Multiconfiguration pair-density functional theory. *J. Chem. Theory Comput.* 2014, 10, 3669–3680.

(40) Gagliardi, L.; Truhlar, D. G.; Li Manni, G.; Carlson, R. K.; Hoyer, C. E.; Bao, J. L. Multiconfiguration pair-density functional theory: A new way to treat strongly correlated systems. *Acc. Chem. Res.* 2017, 50, 66–73.

(41) Carlson, R. K.; Li Manni, G.; Sonnenberger, A. L.; Truhlar, D. G.; Gagliardi, L. Multiconfiguration pair-density functional theory: Barrier heights and main group and transition metal energetics. *J. Chem. Theory Comput.* 2015, 11, 82–90.

(42) Carlson, R. K.; Truhlar, D. G.; Gagliardi, L. Multiconfiguration pair-density functional theory: A fully translated gradient approximation and its performance for transition metal dimers and the

spectroscopy of $Re_2Cl_8^{2-}$. *J. Chem. Theory Comput.* 2015, *11*, 4077–4085.

(43) Bao, J. L.; Sand, A.; Gagliardi, L.; Truhlar, D. G. Correlated-participating-orbitals pair-density functional method and application to multiplet energy splittings of main-group divalent radicals. *J. Chem. Theory Comput.* 2016, *12*, 4274–4283.

(44) Ghosh, S.; Verma, P.; Cramer, C. J.; Gagliardi, L.; Truhlar, D. G. Combining wave function methods with density functional theory for excited states. *Chem. Rev.* 2018, *118*, 7249–7292.

(45) Sharma, P.; Bernales, V.; Knecht, S.; Truhlar, D. G.; Gagliardi, L. Density matrix renormalization group pair-density functional theory (DMRG-PDFT): Singlet-triplet gaps in polyacenes and polyacetylenes. *Chem. Sci.* 2019, *10*, 1716–1723.

(46) White, S. R. Density matrix formulation for quantum renormalization groups. *Phys. Rev. Lett.* 1992, *69*, 2863–2866.

(47) White, S. R. Density-matrix algorithms for quantum renormalization groups. *Phys. Rev. B: Condens. Matter Mater. Phys.* 1993, *48*, 10345–10356.

(48) Marti, K. H.; Reiher, M. The density matrix renormalization group algorithm in quantum chemistry. *Z. Phys. Chem.* 2010, *224*, 583–599.

(49) Kurashige, Y.; Yanai, T. Second-order perturbation theory with a density matrix renormalization group self-consistent field reference function: Theory and application to the study of chromium dimer. *J. Chem. Phys.* 2011, *135*, 094104.

(50) Olivares-Amaya, R.; Hu, W.; Nakatani, N.; Sharma, S.; Yang, J.; Chan, G. K.–L. The ab-initio density matrix renormalization group in practice. *J. Chem. Phys.* 2015, *142*, 034102.

(51) Knecht, S.; Hedegård, E. D.; Keller, S.; Kovyrshin, A.; Ma, Y.; Muolo, A.; Stein, C.; Reiher, M. New approaches for ab initio calculations of molecules with strong electron correlation. *Chimia* 2016, *70*, 244–251.

(52) Hedegård, E. D.; Knecht, S.; Kielberg, J. S.; Jensen, H. J. A.; Reiher, M. Density matrix renormalization group with efficient dynamical electron correlation through range separation. *J. Chem. Phys.* 2015, *142*, 224108.

(53) Roos, B. O.; Lindh, R.; Malmqvist, P.-Å.; Veryazov, V.; Widmark, P.-O. Main group atoms and dimers studied with a new relativistic ANO basis set. *J. Phys. Chem. A* 2004, *108*, 2851–2858.

(54) Roos, B. O.; Lindh, R.; Malmqvist, P.-Å.; Veryazov, V.; Widmark, P.-O. New relativistic ANO basis sets for transition metal atoms. *J. Phys. Chem. A* 2005, *109*, 6575–6579.

(55) Hess, B. A. Relativistic electronic-structure calculations employing a two-component no-pair formalism with external-field projection operators. *Phys. Rev. A: At., Mol., Opt. Phys.* 1986, *33*, 3742–3748.

(56) Vancoillie, S.; Delcey, M. G.; Lindh, R.; Vysotskiy, V.; Malmqvist, P.-Å.; Veryazov, V. Parallelization of a multiconfigurational perturbation theory. *J. Comput. Chem.* 2013, *34*, 1937–1948.

(57) Aquilante, F.; Autschbach, J.; Carlson, R. K.; Chibotaru, L. F.; Delcey, M. G.; De Vico, L.; Fdez. Galván, I.; Ferré, N.; Frutos, L. M.; Gagliardi, L.; Garavelli, M.; Giussani, A.; Hoyer, C. E.; Li Manni, G.; Lischka, H.; Ma, D.; Malmqvist, P. Å.; Müller, T.; Nenov, A.; Olivucci, M.; Pedersen, T. B.; Peng, D.; Plasser, F.; Pritchard, B.; Reiher, M.; Rivalta, I.; Schapiro, I.; Segarra-Martí, J.; Stenrup, M.; Truhlar, D. G.; Ungur, L.; Valentini, A.; Vancoillie, S.; Veryazov, V.; Vysotskiy, V. P.; Weingart, O.; Zapata, F.; Lindh, R. *Molcas 8*: New capabilities for multiconfigurational quantum chemical calculations across the periodic table. *J. Comput. Chem.* 2016, *37*, 506–541.

(58) Keller, S.; Dolfi, M.; Troyer, M.; Reiher, M. An efficient matrix product operator representation of the quantum chemical Hamiltonian. *J. Chem. Phys.* 2015, *143*, 244118.

(59) Knecht, S.; Hedegård, E. D.; Keller, S.; Kovyrshin, A.; Ma, Y.; Muolo, A.; Stein, C. J.; Reiher, M. New approaches for ab initio calculations of molecules with strong electron correlation. *Chimia* 2016, *70*, 244–251.

(60) Keller, S.; Reiher, M. Spin-adapted matrix product states and operators. *J. Chem. Phys.* 2016, *144*, 134101.

(61) Ma, Y.; Knecht, S.; Keller, S.; Reiher, M. Second-order self-consistent-field density-matrix renormalization group. *J. Chem. Theory Comput.* 2017, *13*, 2533–2549.

(62) Freitag, L.; Keller, S.; Knecht, S.; Lindh, R.; Ma, Y.; Stein, C. J.; Reiher, M. *A quick user guide to the SCINE-QCMaquis software suite for OpenMolcas*; https://scine.ethz.ch/static/download/qcmaquis_manual.pdf (accessed Feb 11, 2019).

(63) Östlund, S.; Rommer, S. Thermodynamic limit of density matrix renormalization. *Phys. Rev. Lett.* 1995, *75*, 3537–3540.

(64) Legeza, Ö.; Sólyom, J. Optimizing the density-matrix renormalization group method using quantum information entropy. *Phys. Rev. B: Condens. Matter Mater. Phys.* 2003, *68*, 195116.

(65) Barcza, G.; Legeza, Ö.; Marti, K. H.; Reiher, M. Quantum-information analysis of electronic states of different molecular structures. *Phys. Rev. A: At., Mol., Opt. Phys.* 2011, *83*, 012508.

(66) Pierloot, K.; Tsokos, E.; Roos, B. O. 3p-3d intershell correlation effects in transition metal ions. *Chem. Phys. Lett.* 1993, *214*, 583–590.

(67) Guo, S.; Watson, M. A.; Hu, W.; Sun, Q.; Chan, G. K.-L. N-Electron valence state perturbation theory based on a density matrix renormalization group reference function, with applications to the chromium dimer and a trimer model of poly(p-phenylenevinylene). *J. Chem. Theory Comput.* 2016, *12*, 1583–1591.

(68) Freitag, L.; Knecht, S.; Angeli, C.; Reiher, M. Multireference perturbation theory with cholesky decomposition for the density matrix renormalization group. *J. Chem. Theory Comput.* 2017, *13*, 451–459.